The Carbon-Electrolyte Interface at High Cathodic Voltages

B.E Nilssen[a,1] , A.O. Tezel[a,2] , A.M. Svensson[a]

[a] Department of Materials Science and Engineering, Norwegian University of Science and Technology, 7491 Trondheim, Norway
[1] Current affiliation: Silicon Materials, Elkem AS, Trondheim, Norway
[2] Current affiliation: Graphene Batteries, 0314 Oslo, Norway

Different carbon conductive additives (graphitic and carbon black) were investigated with respect to their electrochemical stability at high voltages, i.e. up to 5V, as next generation cathode materials for Li-ion batteries are expected to operate in the range 4.5-5.0 V. The materials were characterized with respect to crystallinity, surface area and surface structure. Electrodes were fabricated from all materials, and characterized by electrochemical techniques, including galvanostatic cycling, cyclic voltammetry, as well as by *in-situ* X-ray diffraction (XRD) experiments. The results from galvanostatic cycling show that the first cycle irreversible loss correlates with the edge surface area, and that the decomposition products are limiting intercalation and de-intercalation after multiple cycles. Structural damage was observed for the graphitic materials by *in*-situ XRD during the first cycle, no further damage was observed in the subsequent cycles. A means of improving reversibility and preventing structural damage of the carbon materials is finally suggested, based on results obtained with an anion receptor additive.

Introduction

Next generation cathode materials for high-energy Li-ion battery cathodes are expected to operate at voltages up to 5 V. Conductive additives are needed for all known cathode materials, and carbon is regarded as the most suitable material. However, the stability of the carbon conductive additive is challenging at high voltages (i.e. above 4.5 V), as crystalline carbons are known to intercalate the anions of the most commonly used salts (like $LiPF_6$), and furthermore, electrolyte decomposition products will inevitably form on the surface of the carbons. Another application utilizing carbon electrodes at high voltages in similar electrolytes is the so-called dual-carbon battery, where charge storage is actually based on the intercalation of anion and cations, in cathode and anode, respectively, and both electrodes are made from crystalline carbons [1].

The intercalation of PF_6 anions in graphite has been studied in previous works [1,2]. Based on galvanostatic cycling in ethyl methyl sulfone electrolytes (EMS), which is resistant towards oxidation at voltages as high as 5.5 V, Seel and Dahn [1] suggested that PF_6^- intercalates in staged phases. This was suggested based on the appearance of plateaus in the potential curve during galvanostatic cycling, starting at around 4.6 V, in addition to *in situ* (XRD) experiments, which showed significant changes in the

diffraction patterns related to the (002) planes in the graphite structure, including peak shifts and the appearance of a second peak.

In the same study, Seel and Dahn [1] also investigated the reversibility of the anion intercalation for graphite exposed to a more conventional electrolyte based on ethylene carbonate (EC) and diethyl carbonate (DEC) as solvents. Here, the *in-situ* XRD measurements indicated structural damage of the graphite, possibly due to electrolyte decomposition or co-intercalation of solvent molecules [1]. The same behavior has been observed by Märkle *et al.* [2,3], who cycled graphite in propylene carbonate (PC) and EC based electrolytes. Structural degradation of the electrodes was confirmed by SEM, showing particle exfoliation for the most crystalline graphite, as well as by *in-situ* XRD, [2,3]. The less crystalline graphite was more stable in both EC and PC, and the performance of the graphites was generally found to be similar for EC and PC based electrolytes. On the other hand, Wang and Yoshiu [4] observed a significantly lower intercalation potential for the $SBPPF_6$ salt (SBP is spiro-(1,1')-bipyrrolidinium) dissolved in pure PC compared to a mixture of PC and EC for a similar graphite, which was attributed to a strong interaction between EC and PF_6^-. In a recent study, Qi *et al.* [5] reports that for carbon black, a higher degree of crystallinity facilitate the intercalation of anions. Syzdek *et al.* [6] studied the intercalation of anions in carbon blacks by *in-situ* Raman and *in-situ* XRD studies, and found that anion intercalation occurred at potentials lower than observed for graphitic carbons (~ 4.2 V). The anion intercalation also caused structural changes to the materials. With respect to dual carbon cells, Ishihara *et al.* [7] obtained the highest 1st cycle discharge capacities for PF_6^- de-intercalation in 1 M $LiPF_6$ 1:2 EC:DMC (dimethyl carbonate, DMC) electrolyte for the most crystalline graphites. The 1st cycle irreversible capacity loss correlated to the surface area [7].

Zheng *et al.* [8] compared the electrochemical performance at high voltages of various high surface area carbons, like carbon black, Ketjen black and acetylene black in a $LiNi_{0.5}Mn_{1.5}O_4$ cathode. They observed a faster decay of the capacity of electrodes containing graphene and Ketjen black, and proposed that this was due to a higher electrolyte oxidation rate of these high-surface area carbons, and a correlation with electrolyte oxidation with the BET surface area was suggested. The authors further suggested that oxygen functional groups take part in the oxidation reaction. Upon comparison of different types of carbons (acetylene black, carbon black, carbon nanofibers, graphite), however, La Mantia *et al.* [9] did not observe any correlation of irreversible capacity losses and BET surface area. Upon heat treatment of carbon black in Ref. 5, a significant reduction in the irreversible charge was observed, and attributed to removal of surface functional groups, like oxygen groups, or adsorbed water. Qi *et al.* [5] suggest therefore that removal of surface groups by heat treatment, preferably without increasing the crystallinity of the carbon black, will improve the stability of the carbon black.

Although a detailed understanding of the electrolyte oxidation process is still lacking, it is generally agreed both from experimental [10,11] and theoretical [12,13] studies that EC is preferentially oxidized due to the coordination of the EC molecules with the anion. The decomposition of EC results in evolution of CO_2 [10-12], as well as solid decomposition products. Evolution of CO_2 on the $LiNi_xCo_yAl_{1-x-y}O_2$ cathode side was also observed during storage, with EC as the main source [14]. Thus, EC decomposes at the cathode both by chemical and electrochemical mechanisms. For the solid state reaction products oligo(ethylene carbonate) has been observed experimentally [15] and

predicted theoretically [12], and aldehyde and lithium alkyl carbonate was also predicted theoretically [12]. Wang *et al.* [16] observed decomposition of the salt at potentials above 4.9 V for a $LiNi_{1/3}Co_{1/3}Mn_{1/3}O_2$ cathode. In the study of Arakawa *et al.* [11], it was suggested that the anion-intercalated graphite may have a catalytic effect on the decomposition of the cyclic carbonate. Carroll *et al.* [17] compared a composite cathode of $LiMn_{2-x}Ni_xO_{4-\delta}$ with a thin film electrode of the same material, and did not detect any decomposition of either EC or DMC at the thin film electrode at high voltages (5 V). They therefore concluded that it is primarily the carbon conductive additive or the binder phase that reacts with the electrolyte.

In this work three different candidates as carbon conductive additives have been investigated. The carbon materials differ significantly in terms of structure, as one is a low surface area graphite, one is a high surface area, well-graphitized material, and the third is a carbon black with a similar surface area as the latter. The materials were characterized with respect to crystallinity, surface area and surface structure. The carbon black has an edge to basal plane ratio very similar to the low surface area graphite, whereas the high surface area graphite is dominated by edge planes in the surface, with a total surface area similar to the carbon black. Electrodes were fabricated from all materials, and characterized by electrochemical techniques, including galvanostatic cycling, and cyclic voltammetry (multiple cycles), as well as by *in-situ* XRD. Emphasis was put on correlation of the electrochemical characterization and the surface structure, as well as studies of the processes during repeated cycles. Both graphitic materials suffered from structural damage, and means of preventing this structural damage is also suggested.

Experimental

Three types of carbon powder have been studied in this work: KS6 (KS6 L graphite, Imerys), Graphene AO-2 (graphene nanopowder, Graphene Supermarket), and Super P Li (Super P Li, Imerys). The surface area of the powders were determined by nitrogen adsorption by a Tristar II from Micrometrics, which allows for determination of surface areas of basal, edge and defect sites of carbon, based on implementation of a DFT based model for the adsorptive energies, see Ref. 18 for a description. For the SEM investigations of powders and electrodes, a Zeiss Supra, 55 VP, LVFESEM was used. A Bruker D8 Advance diffractometer with Cu-Kα source was applied for the X-Ray diffraction measurements. Electrodes used for the electrochemical characterizations were fabricated by tape casting a slurry containing 90 wt% active material and 10 wt% binder (PVDF from Arkema) with 1-methyl-2-pyrrolidine (NMP, anhydrous, 99.5%, Sigma-Aldrich), as the solvent. The current collector was aluminium foil (0.025 mm thick, 99.45%, from Alfa Aesar). For the galvanostatic cycling experiments, coin cells were assembled with 1M $LiPF_6$ dissolved in 3:7 EC:DMC electrolyte (anhydrous, > 99%, from Sigma Aldrich). The cells were cycled in a MACCOR battery cycler (3 cells from the same cast). For cyclic voltammetry, the electrodes were mounted in a 3-electrode cell, the ECC-REF cell from EL-CELL, using Li as the reference electrode, together with 400-450 µl of electrolyte soaked in a glass fiber separator. The electrodes were cycled at 0.1mV/s between 3.0 and 5.0 V, except for Super P Li, which was cycled up to 5.5 V. The electrolyte additive tris (hexafluoroisopropyle) borate, THFIPB, was purchased from TCI Chemicals. For the *in-situ* XRD experiments, electrodes were casted onto a gold

coated Kapton RSTM X-ray film, and an *in-house* made cell was used, were the working electrode was mounted onto a Beryllium window, transmissive to X-rays. The cell is described in Ref. 19, and is a modified version of the cell design of Leriche *et al.* [20].

Results and Discussion

An overview of the properties of the materials studied is provided in Table 1. As can be inferred from Table 1, the KS6 is well graphitized, with a d002 value close to the theoretical for graphite. The particles are relatively uniform in size. The AO-2 is also well graphitized, and the surface has a high edge to basal plane ratio. The particle size distribution is highly non-uniform, as reflected also by the high specific surface area. The Super P Li carbon black consists of uniformly sized (in the range 40-60 nm), round particles with a low edge to basal plane ratio, typical of carbon blacks, as well as a higher interlayer distance.

TABLE I. Overview of Materials and Properties

Property	KS6	AO-2	Super P Li
Particle size[1]	3 μm (d50)	0.15-3 μm	40-60 nm
Surface area (from N_2 adsorption) [m^2/g]	22.4	57.8	64.9
Ratio edge:basal:defect planes (from N_2 adsorption)	6.8:11.9:3.7	53:2.3:2.5	18.6:32.8:13.5
d002 [Å]	3.357	3.357	3.532
L_c [Å] (from XRD)	649	539	30

[1] From suppliers

Results from galvanostatic cycling, averaged over 3 cells with similar loading, are shown in Figure 1 a)-c) for the 3 materials, with the standard deviation included as error bars. The cells were cycled at increasing rates of 10 mA/g, 20 mA/g, 50 mA/g and 100 mA/g, 2 times at each rate. An example of a typical voltage profile for the KS6 electrode is shown in Figure 1 d). All electrodes exhibit a very high initial charge capacity, related to both anion intercalation and electrolyte oxidation, and a correspondingly high 1st cycle average irreversible capacity of 21.5, 149 and 58 mAh/g for KS6, AO-2 and Super P, respectively. The latter is attributed to extensive oxidation of the electrolyte during the initial charging. For the slow initial cycle, the 1st cycle irreversible capacity correlates well to the edge plane surface area for these three materials, with a ratio of 3.2, 2.8 and 3.1 mAh per m^2 of edge surface area for KS6, AO-2 and Super P, respectively. For KS6 and Super P Li, which has similar ratios of edge to basal surface, this implies that the 1st cycle irreversible capacity loss correlates to the BET surface area, as observed also in Ref. 6. However, based on the high 1st cycle irreversible loss for AO-2, a correlation with the edge plane surface area seems more likely, which is also consistent with other works claiming that oxygen surface groups take part in the oxidation reaction [5,8,9], as

these are primarily associated with the edge planes. The Super P Li material shows a small, but stable discharge capacity, whereas the discharge capacity of KS6 and AO-2 depend strongly on the rate. As electrolyte oxidation is expected to be irreversible, the discharge capacity is assumed to be entirely related to de-intercalation of anions. The relatively high standard deviations of the results for Super P Li are related to the sensitivity of the capacity measured for these electrodes with respect to loading. As particles are small and uniform in size (around 50 nm), the size of the pores of the electrode will be of similar magnitude, and thus less accessible to anions than for example the μm-sized pores of KS6.

Results from galvanostatic cycling at a higher current (120 mA/g) over 50 cycles are shown in Figure 2. Here, the 1st cycle capacity loss is lower, as oxidation rates are reduced at higher rates, as observed also by Märkle *et al.* [2]. No strong correlation to edge or total surface area is observed. The higher discharge capacities at the high constant rate indicate that the intercalation is affected by the formation of surface films.

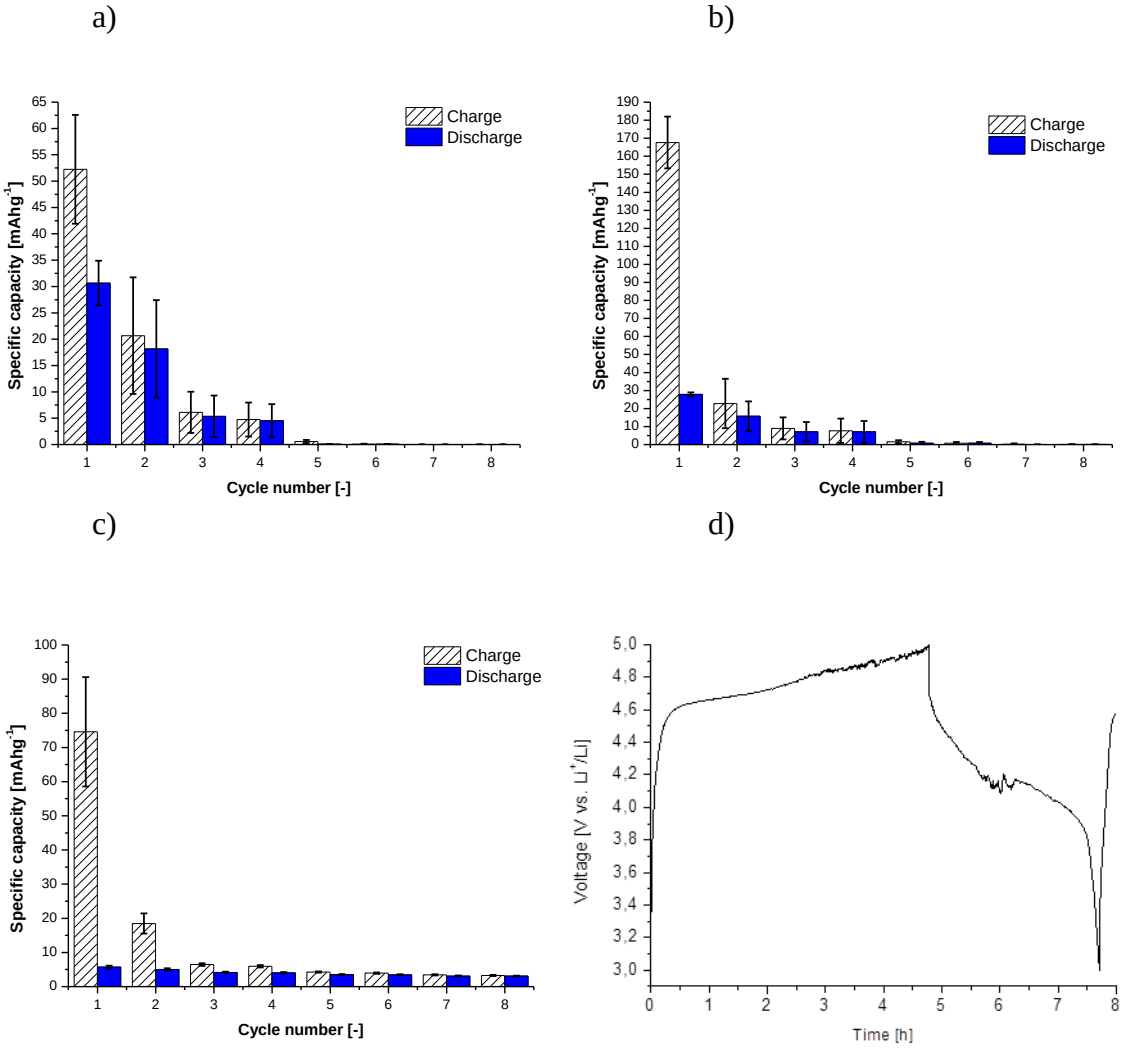

Figure 1. Specific charge and discharge capacity at 10 mA/g (cycle 1 and 2), 20 mA/g, 50 mA/g and 100 mA/g for a) KS6 b) AO-2 and c) Super P Li d) Voltage profile obtained during initial slow galvanostatic charge/discharge at 10 mA/g for KS6.

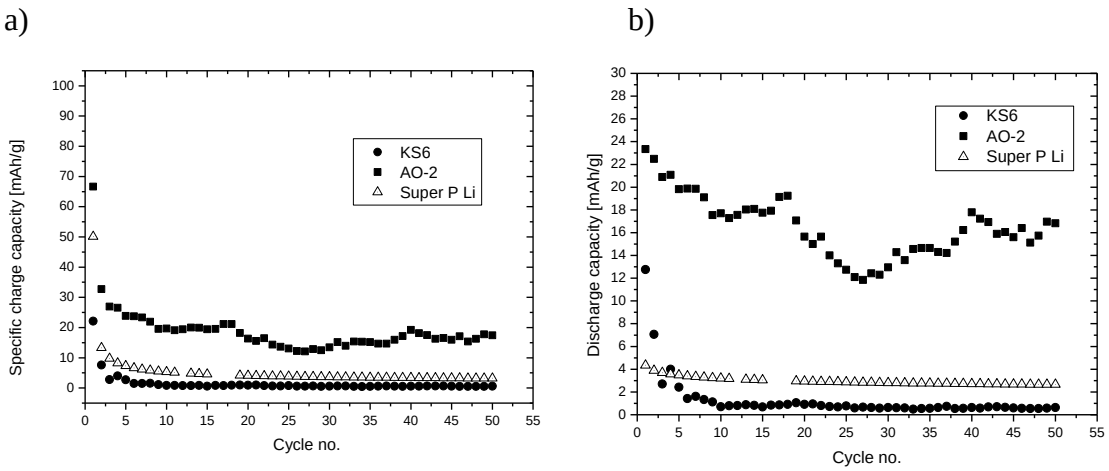

Figure 2. Specific capacity obtained during cycling at 120 mA/g (50 cycles) a) Specific charge capacity b) Specific discharge capacity.

As can be seen from Figure 1d), the 1st voltage profile for KS6 is highly irregular, clearly indicating possible exfoliation of the material during cycling. The same applies to AO-2, whereas the voltage curves for Super P Li were all smooth (not shown here). As graphitic materials are known to intercalate anions in this potential range, cycling performance of the KS6 and AO-2 materials was studied further by *in-situ* X-ray diffraction, recorded during galvanostatic cycling, starting by two cycles at 10 mA/g and the two at 20 mA/g, in the potential range of 3-5 V. The X-ray patterns obtained during the first two cycles are shown in Figure 3 a) and b) for KS6 and AO-2, respectively. Changes in the diffraction spectra are observed almost immediately after the increase in potential, and a significant shift and broadening of the (002) peak is observed for both materials, clearly indicating an enlarged interlayer spacing due to intercalation of anions. For KS6, a new peak appeared in addition to the characteristic (002) peak, indicating staged intercalation, similar to previously reported results [1]. The stage index was estimated to 3.39 at 5 V. Compared to the work by Seel and Dahn [1], who cycled graphite electrodes *in-situ* in $LiPF_6$/EMS electrolyte, both the stage index, and the discharge capacity at 5 V (28 mAh/g) are lower. This is expected, as EMS is resistant to oxidation at these voltages, and will not form surface films which prevent the intercalation of anions. Similar findings were reported for the EC:DEC solvent [1], which is even more susceptible to oxidation than EC:DMC [12] and for PC:DMC electrolyte [2].

For the AO-2 material, the development of a second peak after the initial full cycle is not observed, and might simply be related to the higher noise level of these measurements, or the fact that the material is less crystalline, or has more micropores.

Figures 4 a)-f) show the shifts in the peak positions during the initial cycle up to 5 V for KS6 and AO-2 (Figure 8 a) and b)), a comparison of the peaks for fully charged cells, i.e at 5 V for KS6 and AO-2 (Figure 8c) and d)) and a comparison of the peaks for fully discharged cells, i.e at 3 V for KS6 and AO-2 (Figure 8e) and f)). The peak shift is observed from around 4.6 V for both materials, which corresponds to the peak shifts observed by Märkle *et al* [2] for SFG44.

a)

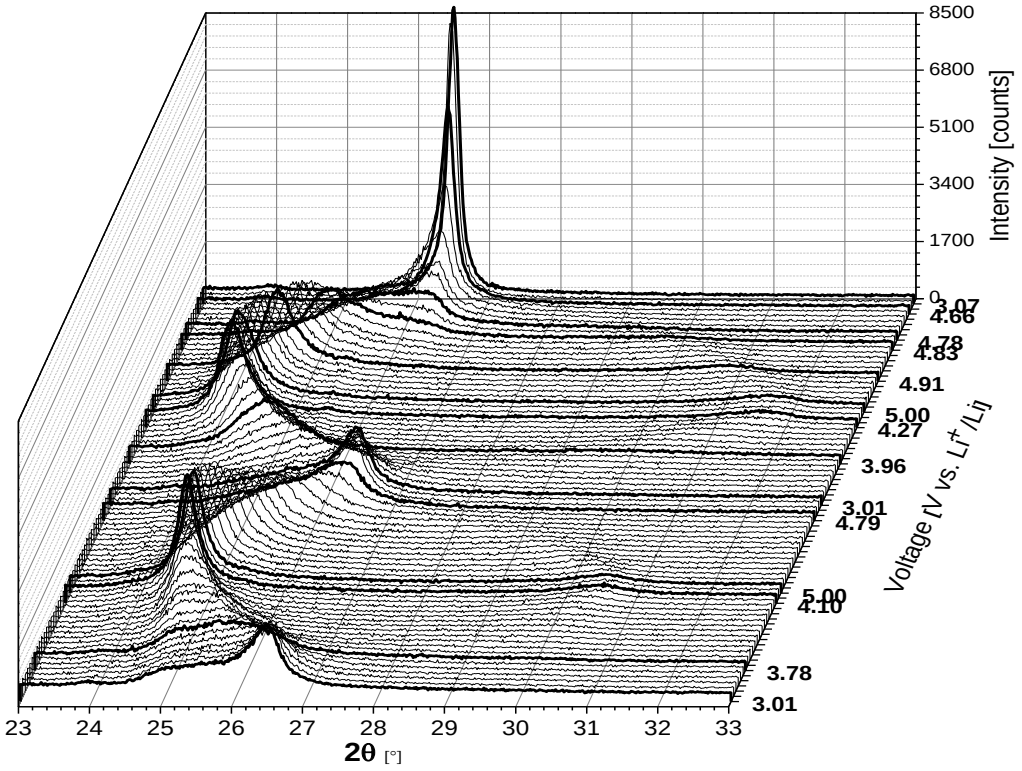

b)

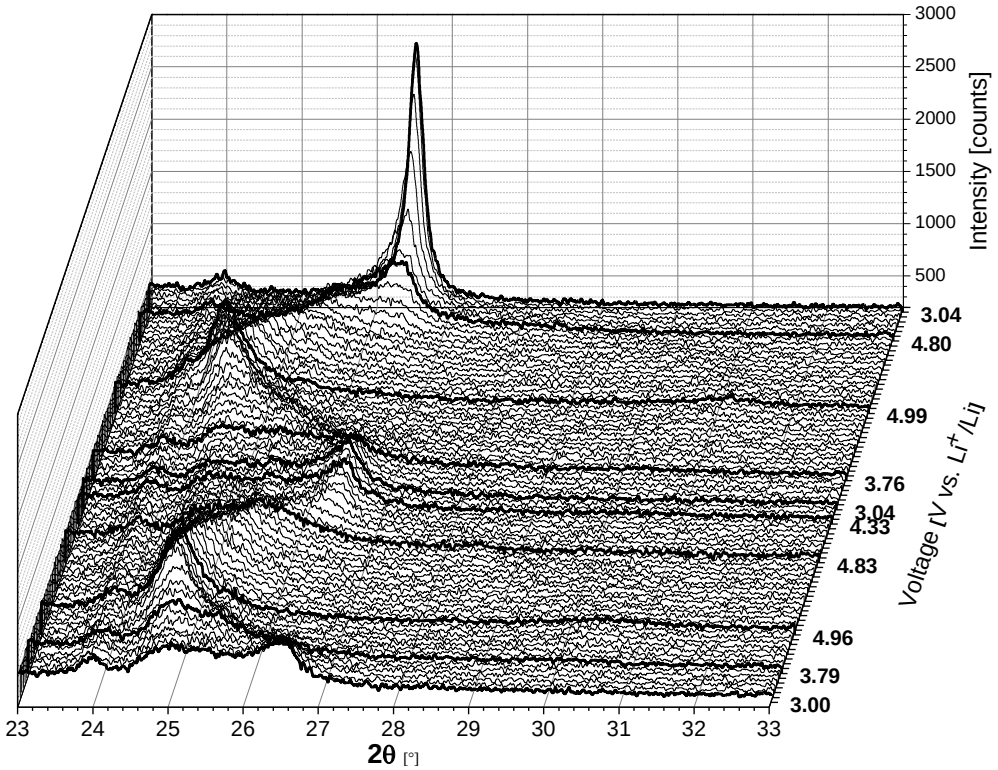

Figure 3. *In-situ* XRD patterns recorded during galvanostatic cycling (2 cycles) at 10 mA/g a) KS6 b) AO-2.

After completion of the first cycle, the X-ray diffraction scans are more or less overlapping upon completion of the next 3 cycles (Figures 4e) and f)), showing that the structural changes of both materials are irreversible, and occurring during the initial intercalation. Structural damage of the graphite was also observed by Seel and Dahn [1] for the EC:DEC electrolyte, and attributed to electrolyte films formed on the surface or co-intercalation of electrolyte compounds. Märkle *et al.* [2] observed structural damage only for the most crystalline graphite, SFG44 with relatively large particles (d50 = 23.9 μm), and not for the slightly less crystalline material SFG6 of smaller particles (d50 = 3.3 μm) in an 1M $LiPF_6$ PC:DMC electrolyte.

During repeated cycles, we observe that the peak shift at 5 V is reduced, showing that the oxidation products prevents intercalation of anions in the cycles 2-4 (Figures 4 c) and d)). This shows that the films formed by electrolyte decomposition are not passivating the surface, in agreement with the data from galvanostatic cycling. Increasing the charging current to 20 mA/g also lead to further reduction and broadening of the peaks (Figure 4 c) and d)), in line with the reduced capacity at higher rate, observed also upon galvanostatic cycling

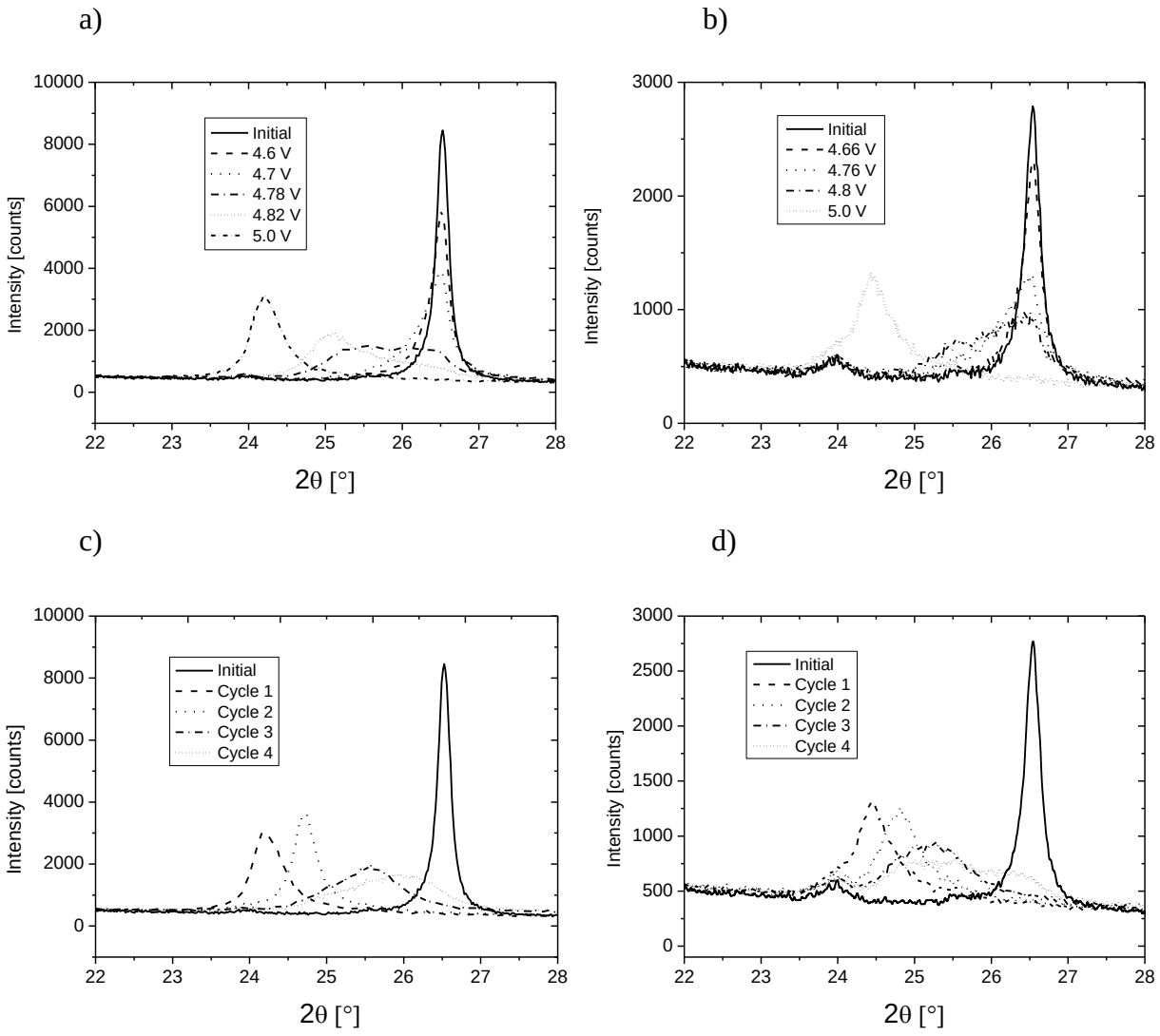

e) f)

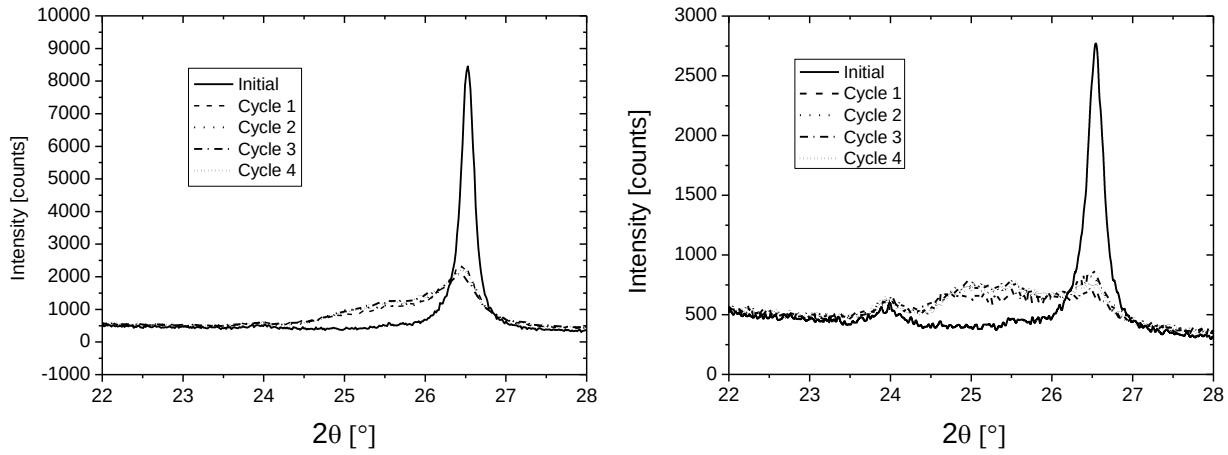

Figure 4. X-ray scans obtained during a) Initial charging, KS6 b) Initial charging, AO-2 c) KS6 at 5.0 V, cycle 1-4 d) AO-2 at 5.0 V, cycle 1-4 e) KS6 at 3.0 V, cycle 1-4 f) AO-2 at 3.0 V, cycle 1-4.

Cyclic voltammograms of all materials are shown in the Figures 5 a)-e). The voltammograms for the graphitic materials (Figures 5a) and b)) at a cut-off voltage of 4.7 V show high currents during the initial cycle, but close to reversible behavior in the subsequent cycles. Three reduction peaks are seen, which may be attributed to de-intercalation of anions. All voltammograms of the graphitic materials show a steady increase of the current starting from below 4.0 V in the first cycle, which however, disappears in the subsequent cycle, thus indicative of an electrolyte oxidation process that partly passivates the surface, as also observed by others [2,3]. Most probably this process involves EC, as EC is known to be preferentially oxidized [10-13]. When the cut-off voltage is increased to 5 V, the current becomes very noisy above 4.7 V, in particular for the KS6 electrode; a clear indication of structural damage. The currents are decreasing during multiple cycles, and the highly irregular reduction peaks are shifted towards more negative potentials. It is likely that the structural damage experienced by the electrode in the voltage range 4.7-5.0 V exposes fresh surface, which is subsequently oxidized. In addition, the decomposition products do not appear to completely passivate the surface upon repeated cycles, but creates an increasing barrier for de-intercalation of the anions upon repeated cycling. This is in agreement with the results from the *in-situ* XRD, Figures 4e) and f). The voltammogram of the AO-2 electrode (Figure 5d)) exhibits similar qualitative features. The initial current is higher compared to the currents in the subsequent cycles, and also higher than for the KS6 electrode, in agreement with the high 1st cycle irreversible loss observed during galvanostatic cycling. The shifts of the reduction peaks are less, indicating a slightly more reversible behavior than the KS6 electrode, also in agreement with the *in-situ* XRD results. The cyclic voltammogram of the Super P Li electrode, Figure 5e), differs from the graphitic materials in that no distinct reduction peak is observed, although the galvanostatic cycling showed a finite discharge capacity. As for KS6 and AO-2, the current during the 1st cycle is higher, but only from around 4.7 V, were the current increases sharply, due to intercalation of anions. Anion intercalation has previously been verified in carbon blacks [6], but starting at even lower potentials. The two oxidation peaks are indicative of staged intercalation. The current decreases during subsequent cycles, but the films formed are apparently not

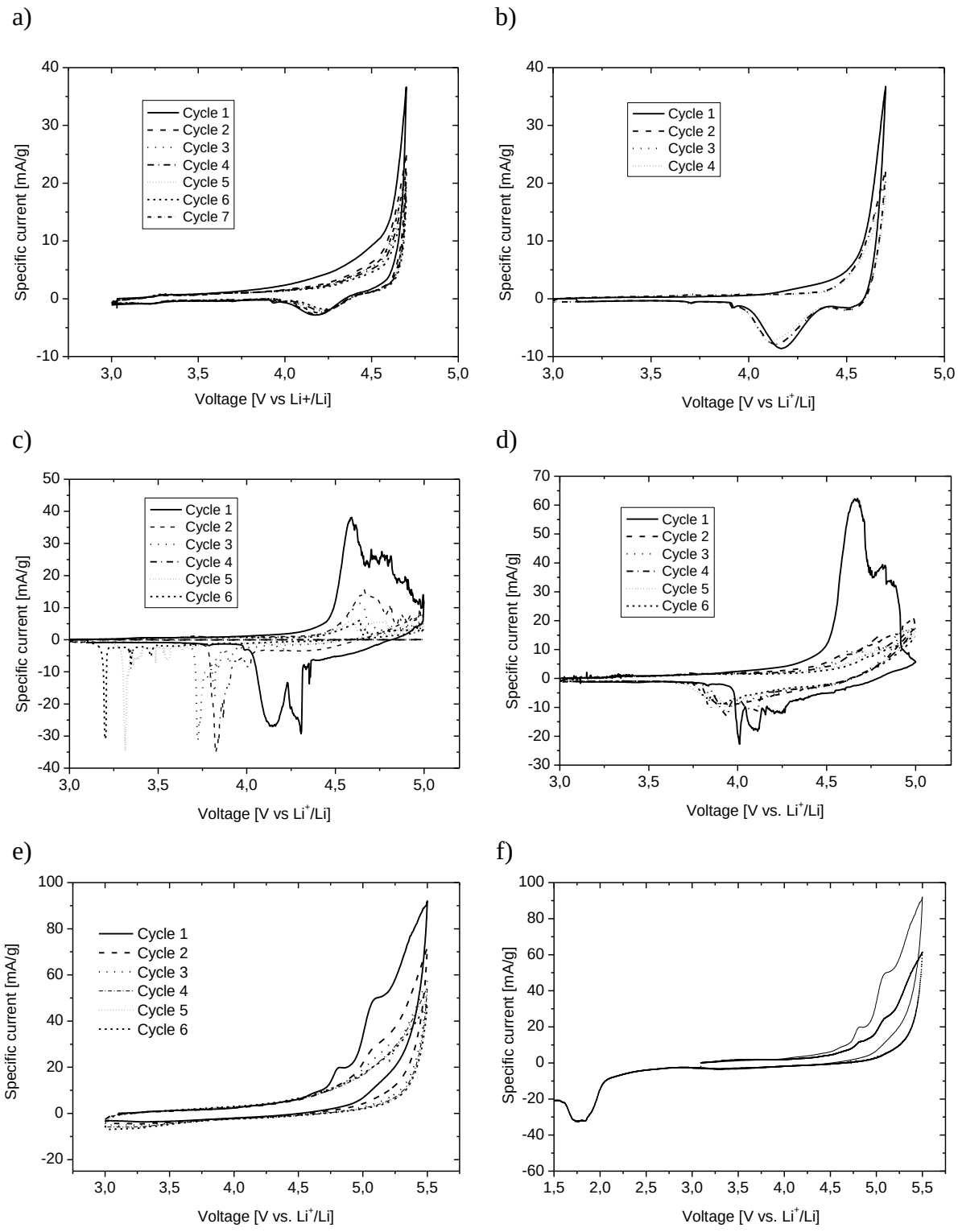

Figure 5. Cyclic voltammograms obtained at 0.1 mA/g for a) KS6 with cut-off voltage 4.7 V b) AO-2 with cut-off voltage 4.7 V c) KS6 with cut-off voltage 5.0 V d) AO-2 with cut-off voltage 5.0 V e) Super P, with cut-off voltage 5.5 V f) Super P with lower cut-off voltage 1.5 V.

passivating the surface very well, meaning that there is a risk of continuous build-up of oxidation products during operation of a cathode. To investigate the absence of the reduction peak, one electrode was cycled to a much lower cut-off voltage, as shown in Figure 5 e). Here a distinct reduction peak is observed at a potential as low as 1.8 V. It is however known that in this potential range (1.5-2.5 V), reduction of electrolyte impurities like H_2O, might occur, which might also be the origin of the observed reduction peak.

In order to investigate the possibility of improving the stability of the carbon at high cathodic voltages, an electrolyte additive, the THIFPB, was added to the electrolyte at a concentration of 0.025 M (1 wt%). Cyclic voltammograms for KS6 and AO-2 recorded at 0.1 mV/s are shown in Figure 6 a) and b). Whereas improved reversibility is observed for KS6, the most striking result is the reversible behavior of AO-2 after the initial cycle. The reason for this not understood, and is subject to further investigations. The THFIPB additive is known to have a high F^- affinity, and will bind to an F^- and accelerate the decomposition of the salt according to

$$PF_6^- + \text{THFIPB} \rightarrow \text{THFIPB} - F^- + PF_5 \qquad [1]$$

Possible causes for the improved reversibility might therefore be related to the presence of PF_5, and chemical reactions with surface oxygen or water associated with surface oxygen groups, or chemical reactions with EC, and the corresponding formation of protective surface films. Another interesting observation is that the current during the 1st cycle is suppressed below the onset potential, unlike the steady increase of the current observed in Figures 5c) and d).

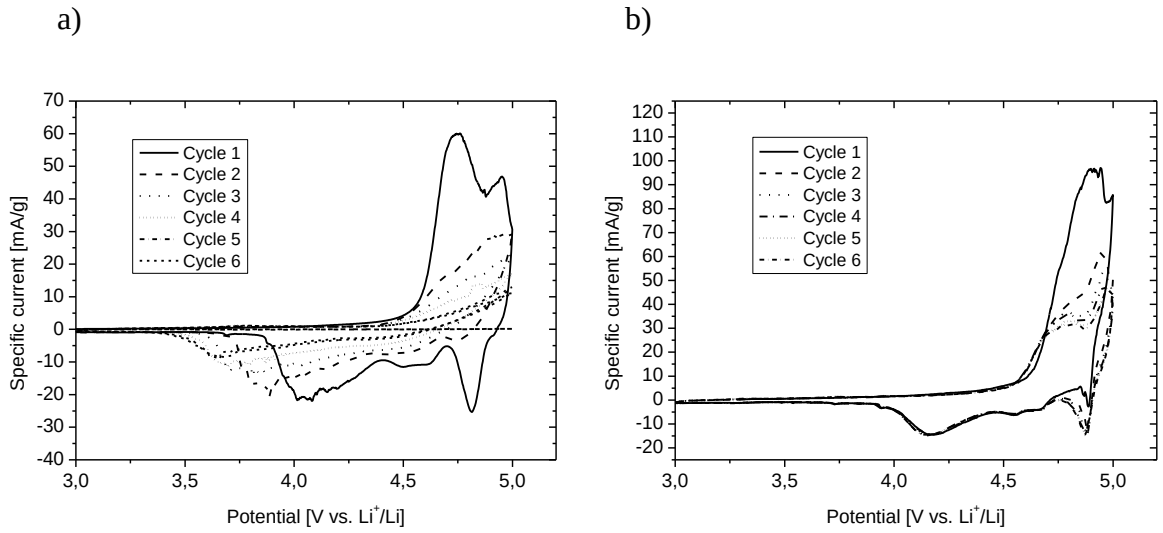

Figure 6. Cyclic voltammograms obtained at 0.1 mA/g with 0.025 M THFIPB added to the electrolyte a) KS6 with cut-off voltage 5.0 V b) AO-2 with cut-off voltage 5.0 V

Conclusions

The stability of carbon materials at high cathodic voltages was investigated. High irreversible capacities were observed during the initial charging, and found to correlate with the edge plane surface area of the materials. Irreversible structural damage of the

graphitic carbons was observed upon cycling above 4.7 V, but only during the initial cycle. The film formed due to decomposition reactions is not passivating the surface. Addition of the anion receptor THFIPB was found to improve the reversibility, in particular for the high surface area graphitic carbon AO-2.

Acknowledgments

The Norwegian University of Science and Technology is acknowledged for the financial support of this work. Julian Tolchard is acknowledged for assistance with the in-situ XRD experiments, and Carl Erik Foss for assistance with the BET measurements.

References

1. J.A. Seel and J.R. Dahn, *J. of Electrochem. Soc.,* **147**(3), 892-898 (2000).
2. W. Märkle, J-F Colin, D. Goers, M.E. Spahr, P. Novak, *Electrochimica Acta,* **55,** 4964-4969 (2010).
3. W. Märkle, N. Tran, D. Goers, M. Spahr, P. Novak, *Carbon*, **47,** 2727-2732 (2009).
4. H. Wang and M. Yoshiu, *Chem. Comm.*, **46,** 1544-1546 (2010).
5. X. Qi, B. Blizanac, A. DuPasquier, P. Meister, T. Placke, M. Oljaca, J. Li, M. Winter, *Phys. Chem. Chem. Phys.*, **16,** 25306-25313 (2014).
6. J. Syzdek, M. Marcinek, R. Kostecki, *J. Power Sources,* **245,** 739-744 (2014).
7. T. Ishihara, M. Koga, H. Matsumoto, M.Yoshio, *Electrochem. Solid State Letters,* **11,** A72 (2008).
8. J. Zheng, J. Xiao, W. Xu, X. Chen, M. Gu, Li, Xiaohong., Zhang, J-G., *J. Power Sources,* **227,** 211-217 (2013).
9. F. La Mantia, R.A. Huggins, Y. Cui, *J. Appl. Electrochem.* **43, 1-7** (2013).
10. F. Joho, P. Novak, *Electrochim. Acta,* **45,** 3589-3599 (2000).
11. M. Arakawa, J-I Yamaki, *J. Power Sources*, **54,** 250-254 (1995).
12. L. Xing, and O. Borodin, *Phys. Chem. Chem. Phys.*, **14,** 12838-12843 (2012).
13. L. Xing, C. Weishan, C. Wang, F. Gu, M. Xu, C. Tan, J. Yi, *J. Phys. Chem.*, **113,** 16596-16602 (2009).
14. M. Onuki, S. Kinoshita, Y. Sakata, M. Yanagidate, Y. Otake, M. Ue, M. Deguchi, *J. Electrochem. Soc.* **155**(1), A794-A797 (2008).
15. L. Yang, B. Ravdel, B.L. Lucht, *Electrochem. and Solid State Letters* , **13**(8), A95-A97 (2010).
16. Z. Wang, Y. Sun, L. Chen, X. Huang, X., *J. Electrochem. Soc.*, **151**(6), A914-A921 (2004).
17. K.J. Carroll, M.C. Yang, G.M. Veith, N.J. Dudney, Y.S. Meng, *Electrochem. and Solid State Letters* , **15**(5), A72-A75 (2012).
18. J. Olivier, Adsorption of carbons, 2008: p. CH7.
19. Z. Haitao, M. Einarsrud, M., F. Vullum-Bruer, *J. Power Sources,* **238,** 478-484 (2013)
20. J.B. Leriche, S. Hamelet, J. Shu, M. Mocrette, C. Masquelier, G. Ouvrard, M. Zerrouki, P. Soudan, S. Belin, E. Elkaïm, F. Baudelet, *J. Electrochem. Soc.*, **157,** A606-A610 (2010)